Microchimica Acta (2020) 187:530
https://doi.org/10.1007/s00604-020-04515-0

ORIGINAL PAPER

Paper-based electrochemiluminescence determination of streptavidin using reticular DNA-functionalized PtCu nanoframes and analyte-triggered DNA walker

Yuzhen Huang[1,2] · Lina Zhang[3] · Sibao Zhang[4] · Peini Zhao[2] · Li Li[2] · Shenguang Ge[1] · Jinghua Yu[2]

Received: 5 May 2020 / Accepted: 18 August 2020

Abstract

A paper-based electrochemiluminescence (ECL) biosensor characterized by the signal amplification of reticular DNA-functionalized PtCu nanoframes (DNA-PtCuTNFs) and analyte-triggered DNA walker was developed for sensitive streptavidin assay. Silver microflower functionalized paper-based sensing platform was prepared to fix the hairpin strand (S1). With addition of the streptavidin, plenty of DNA walkers consisting of the walking strands (S2) labeled with biotin and streptavidin were established, which protected S2 from digestion via the terminal protection mechanism. The sequential introduction of the DNA walker and capture probe initiated the hairpin structure opening of S1 and strand displacement reaction (SDR) happening, causing the S2 release. Subsequently, S1 hybridized with S3. The free S2 further hybridized with adjacent S1 to trigger the next cycle. After multiple cycles, the DNA-PtCuTNFs, the fire-new signal enhancer, with remarkable peroxidase activity, were successfully attached onto the paper electrode via metal-catalyst-free click chemistry. Based on the SDR of the DNA walker and the catalysis of DNA-PtCuTNFs, a significantly boosted ECL signal of luminol was obtained. Under the optimal conditions, the developed sensor for streptavidin assay exhibited a low detection limit of 33.4 fM with a linear range from 0.1 pM to 0.1 μM.

Keywords DNA walker · PtCu tripyramidal nanoframes · Electrochemiluminescence · Click chemistry

Introduction

Proteins play a key role in most life activities. Especially, streptavidin (SA), a protein that is isolated from bacteria Streptomyces avidin, still maintains its activity in extreme environments. And this stable SA possesses the high affinity with biotin, promoting its application in medical, biological, and analysis fields. In order to play its role effectively, ultrasensitive SA detection is a first essential step for obtaining high yield and purity of SA from Streptomyces avidin. Recently, many technologies have been developed for the detection of SA. For instance, Li et al. have firstly introduced the molecular translators into protein assay. Gold nanoparticles were used as the scaffold for binding-induced DNA strand displacement, achieving the fluorescent detection of SA successfully [1]. In order to improve the sensitivity,

Electronic supplementary material The online version of this article (https://doi.org/10.1007/s00604-020-04515-0) contains supplementary material, which is available to authorized users.

✉ Li Li
jnlil2014@163.com

✉ Shenguang Ge
chm_gesg@163.com

[1] Collaborative Innovation Center of Technology and Equipment for Biological Diagnosis and Therapy in Universities of Shandong, Institute for Advanced Interdisciplinary Research, University of Jinan, Jinan 250022, People's Republic of China

[2] Collaborative Innovation Center for Green Chemical Manufacturing and Accurate Detection, School of Chemistry and Chemical Engineering, University of Jinan, Jinan 250022, People's Republic of China

[3] Shandong Provincial Key Laboratory of Preparation and Measurement of Building Materials, University of Jinan, Jinan 250022, People's Republic of China

[4] Chemical Technology Academy of Shandong Province, Qingdao University of Science and Technology, Jinan 250014, People's Republic of China

Published online: 29 August 2020

graphene oxide was employed to adsorb fluorescent-labeled DNA for ultrasensitive SA assay by Xiang's groups [2]. Huang and co-workers further proposed a novel platform based on MoS_2 nanosheet for fluorescence signal amplification to shorten preparation process and reduce cost, because, compared with graphene, MoS nanosheets can be facilely synthesized in large scale and directly dispersed in aqueous solution without the extra treatment with surfactants or oxidation [3]. These fluorescence sensors exhibit high sensitivity and selectivity, but it is limited by expensive fluorescence detection equipment. So, a square-wave voltammetry based on the carbon paste electrode made of 70% graphite powder and 30% mineral oil was also proposed for SA assay by Kizek's group [4]. Despite the approach are simple and inexpensive, and can be routinely performed by technicians, it cannot meet the demand for trace sample. Therefore, it is urgent and pivotal, but full of challenge to exploit a simple, cheap, high-efficiency, and innovative analytical method for trace SA assay.

Electrochemiluminescence (ECL) sensing analytical method [5–8], as the ideal combination of electrochemical and luminescence method, had its unique characteristic of simplified setup, high reproducibility, low background signal, etc. So far, plenty of ECL signal amplification strategies have been studied to pursue splendid sensitivity detection, such as polymerase chain reaction, and enzyme-catalyzed amplification technology. Nevertheless, affected by cumbersome thermal-cycling course and relatively complicated procedure or design, these avenues suffered from hindrance. Due to its high chemical stability, the facile synthesis of DNAs, the remarkable locomotion, and controllability, the artificial DNA machines relying on DNA and small molecules as the fuels to conduct the repetitive mechanical operations [9–11], as a promising alternative, were taken into account. Herein, in consideration of the streptavidin (SA) possessing high affinity with biotin to form a stable biotin-streptavidin binding system [12], an autonomous DNA walker assembled by the walking strands labeled with biotin (S2-biotin) and target SA was designed. With the movement of DNA walker propelled by toehold-mediated strand displacement reaction (SDR) of probe, the signal was tremendously amplified. Noticeably, in comparison with traditional DNA machines, the movement process did not need any assistance of stimuli and external energy, which avoided the interference from metal ions or enzymes as well as the extra operation. Meanwhile, the proposed signal amplification strategy overcame the frequent deficiency of protein conversion with enzyme cleavage or polymerization in traditional detection of protein, thus it being desirable to have highly efficient application in protein analysis.

Furthermore, nanomaterials emerged distinct superiority in the fabrication of ECL biosensors on account of its superiorities like good biocompatibility and high specific surface area [13–16]. Among them, PtCu tripyramidal nanoframes (PtCuTNFs), as a kind of prominent Pt-based bimetallic nanomaterials [17–19] exhibiting superior catalytic property, high conductivity, and good stability, have been widely concerned and researched. Especially, owing to the PtCu nanomaterials possessing highly open nanostructure composed of interlinked branches units, its electrocatalytic performance and specific surface area could be further improved. Additionally, with the existence of Pt element, PtCuTNFs could accelerate the decomposition of H_2O_2 and produce reactive oxygen species (ROS). Thus, PtCuTNFs could be an ideal candidate for the assembly of signal label, showing great promise in improvement of the ECL signal response of luminol-H_2O_2 co-reaction system.

An appropriate sensing platform is also the critical factor for high-performance ECL biosensor. Portable paper-based chip [20–22] featuring with inexpensive, abundant, portability, retrievability, designability, foldability, and hydrophilicity showed a powerful competitive advantage over other traditional sensing platforms such as glassy carbon electrode, FTO, ITO, Si, and glass, since it was first reported by Whitesides' group [23]. Especially, the capillary action produced by the paper cellulosic fibers can drive fluid transport without external power sources, simplifying the fabrication process, minimizing the scale, and reducing the expense, which is especially beneficial for microanalysis [24]. Yet, the presence of the cellulose matrix also brings about some difficulties, such as poor conductivity [25]. As for this issue, silver materials, as one of the best conductive materials, were considered to modify cellulose matrix of the chip [26]. Restricted by the fact that paper could not withstand the high temperature, high pressure, extreme pH, and strong oxidant, a simple, facile, and non-pollution chemical reduction method was adopted for in situ growing silver micromaterials with 3D flower-like structure on the paper working electrode (AgMFs-PWE). Therefore, the prepared AgMFs-PWE with large surface area and excellent electroconductibility could promote electron transfer and increase the loading quantity of molecules and was chosen as the sensing platform, which laid a strong foundation for the proposed ECL biosensor.

Herein, a paper-based ECL determination of streptavidin using reticular DNA-functionalized PtCu nanoframes (DNA-PtCuTNFs) and analyte-triggered DNA walker was proposed. Concretely, the analyte was firstly linked with biotin-S2 to assemble the DNA walker by SA-biotin interactions. Through the DNA hybridization, the hairpin structure of S1 was opened by S2 of the walker, which further triggered the SDR proceeding between S2 and dibenzocyclooctyne-modified capture probe (S3-DBCO), resulting in the movement of the DNA walker. Afterwards, the reticular nanoarchitectures combined by PtCuTNFs and azide-modified strand S4 (S4-N_3) were connected with the S3 via click chemistry reaction between DBCO and N_3.

Noteworthily, the click chemical ligation proceeded fluently and smoothly between DBCO and N_3 groups without any catalyst, avoiding interference from coexisting biomolecules and groups due to the sluggishness of DBCO and N_3. Under the optimal conditions, the ECL biosensor exhibited a lower detection limit of 33.4 fM. Therefore, the proposed analyte-triggered DNA walker provided a promising tool to construct efficient and rapid analytical strategy for protein.

Experimental

Ethics statement

All methods were performed in accordance with the relevant guidelines and regulations. The serum samples in this study were obtained from Shandong Tumor Hospital in accordance with institutional ethical standards laid down in the 1964 Declaration of Helsinki and its later amendments.

Design of the 3D paper-based device

The proposed paper-based device was prepared on basis of our previous work with slight modification [27] (detailed procedure can be found in Supporting Information). As shown in Scheme 1B, the whole paper-based device was composed of a working pad, a counter pad, a multipass pad, a hollow channel pad, and an absorptive pad. The 1 mm of width of unprinted lines between different tabs was set as a flexible interval to accurately fold the device. On the green working pad, a circular hydrophilic area was used for screen-printing the working electrode (WE) and assembling the ECL biosensor (Scheme 1A). Carbon counter electrode (CE) and Ag/AgCl reference electrode (RE) were stencil-printed onto the bottom of the circular hydrophilic zone in the counter pad, respectively. Before measurement, the opposite pad was folded under the working pad (Scheme 1D), which ensured the hydrophilic regions of the two pads well overlapping. When the buffer was added into the hydrophilic regions, the electrochemical cell was formed, achieving the signal detection.

Reduplicative washing steps that could lead to the excessive consumption of time, manpower, and material resources, are one of frequent deficiencies in the paper-based device. Herein, in order to overcome the deficiency, a three-channel structure (numbers 1–3, Scheme 1A) was introduced to control the length of the fluid passageway. The cleaning liquid dropped at area I would arrive at the working electrode in three times on the basis of the differences passageway, which achieved the multiple auto-cleaning of the working electrode with one drop of buffer. The detailed operation of cleaning process was as follows: first, the purple hollow channel pad was put in the place between the red multi-channel pad and the green working pad and ensured the doublication among areas II, III, and IV (Scheme 1C). Meanwhile, the absorptive pad was under the working pad. When the cleaning buffer was added into the area

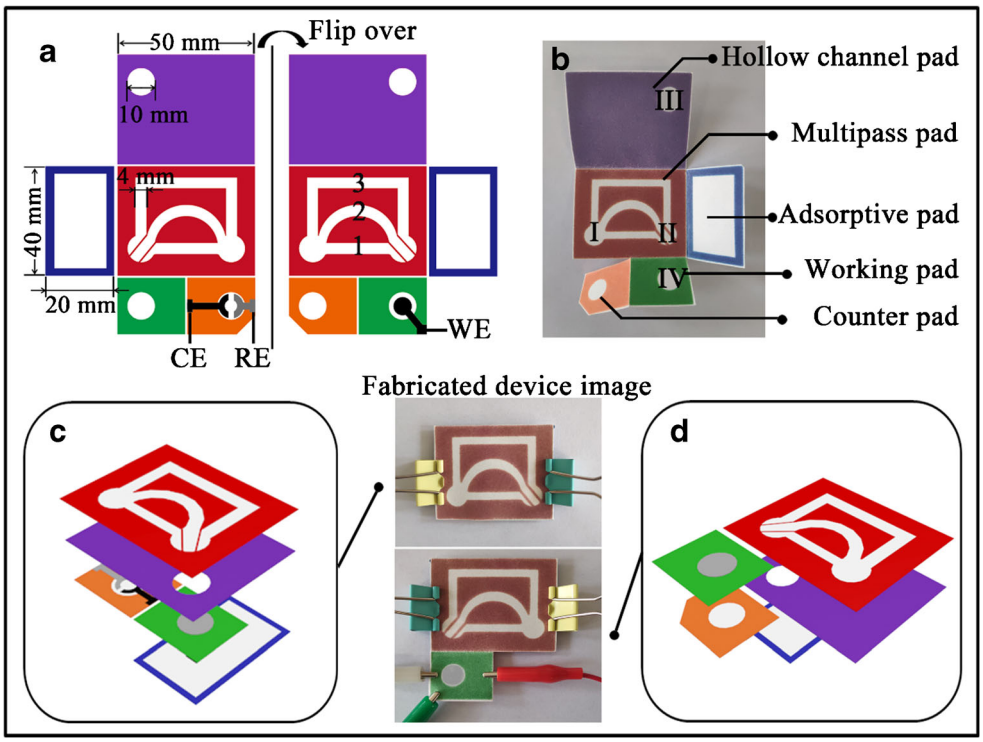

Scheme 1 (**a**) Wax-printing pattern of the device. (**b**) The photograph of the device. (**c** and **d**) The 3D pattern of the paper-based device

I, the buffer would flow to the area II through three channels with different lengths on account of the capillary force generated from the hydrophilic network of cellulose fibers. With the help of the weight, the liquid reaching the area II would flow to the electrode surface along the hollow channel III. The buffer assisted by capillary action was rapidly diffused over the electrode surface and was eventually assimilated by the bottom adsorptive pad, achieving the lateral and vertical cleaning of PWE automatically. In order to explore the cleaning performance of the proposed chip, the ECL responses of the biosensor in the different cleaning mode have been measured. In traditional cleaning method (Fig. S4), the signal intensity obtained obvious decrease on account of the insufficient cleaning (Fig. S5). However, the longitudinal cleaning process provided a better result compared with the traditional method. Its signal was still slightly less than the auto-cleaning method. Because the auto-cleaning method simultaneously completed both horizontal and vertical cleaning processes, the cleaning of the electrode is completely sufficient. According to the relative standard deviation, its signal intensity was significantly more stable, indicating the superiority of the designed chip.

Preparation of AgMFs-PWE and DNA-PtCuTNFs

AgMFs-PWE was synthesized similarly to the literature preparation [28]. The detailed preparation procedure was represented in the Supporting Information.

The synthetic procedure of DNA-PtCuTNFs mainly involves three steps (Scheme 2C). First, PtCuTNFs were synthesized according to a reported method [29] with slight modifications (the detailed synthesis method shown in Supporting Information). Second, 40 μL of 1 μM S4 solution was added into equal volume of PtCuTNFs buffer solution and oscillated at 4 °C for 12 h, resulting in the effective binding of S4 to PtCuTNFs. Third, the mixture was sequentially incubated at 37 °C for 4 h. To remove excess reactants, the solution was centrifuged with buffer at least 4 times to obtain DNA-PtCuTNFs.

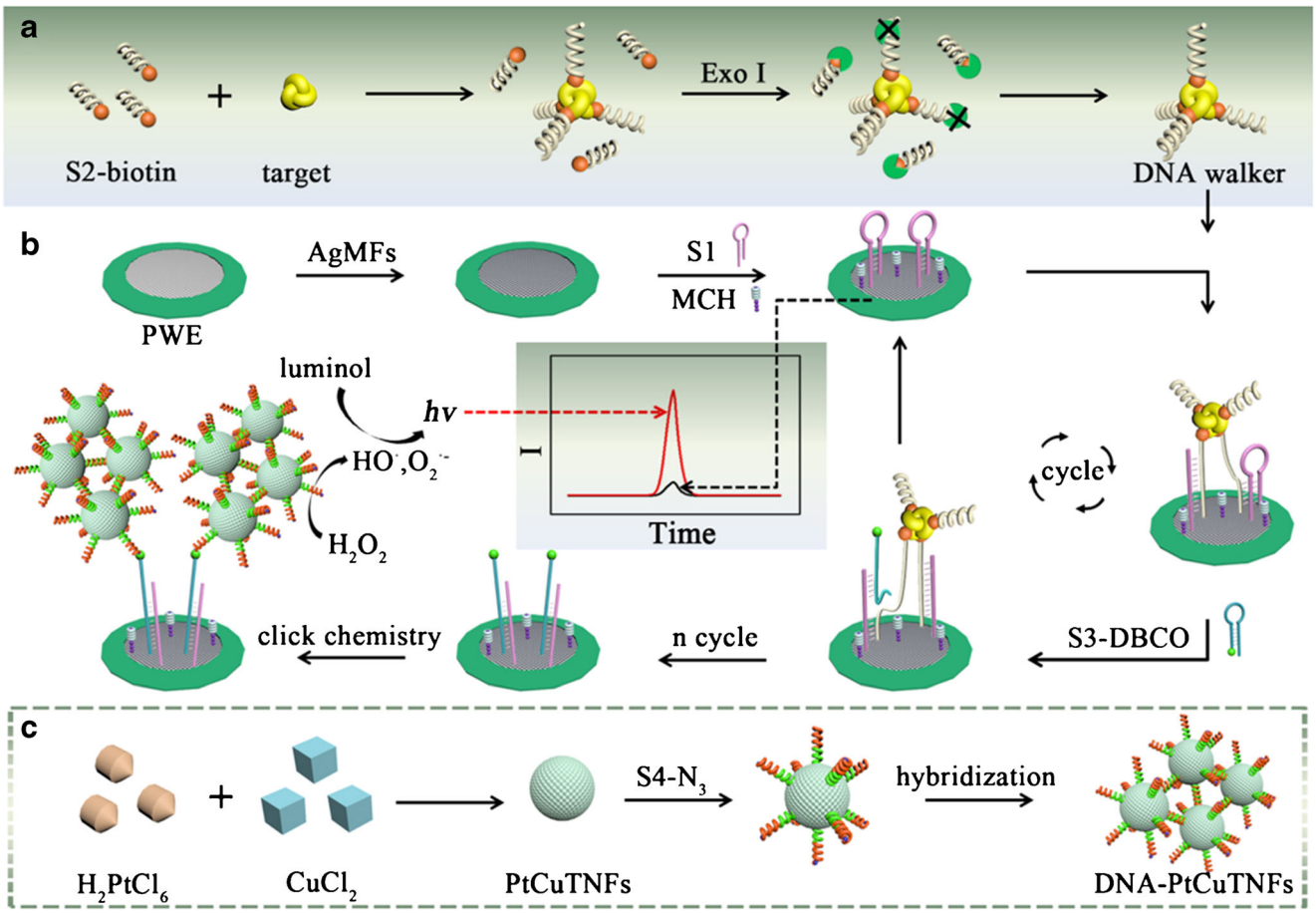

Scheme 2 (**a**) Preparation of the analyte-triggered DNA walker. (**b**) Preparation and analysis process of the paper-based device. (**c**) Synthetic procedure of the DNA-PtCuTNFs

Fabrication of the ECL biosensor

The fabrication of the paper-based ECL biosensor was schematized in Scheme 2. Concretely, 40 μL of S1 (2.5 μM) was firstly dripped on the as-prepared AgMFs-PWE and incubated overnight. The device was folded into the configuration as Scheme 1C to finish the electrode cleaning. After drying at room temperature, 20 μL of 1 mM 6-hydroxy-1-hexanethiol (MCH) solution was used for sealing remaining non-specific sites of the AgMFs-PWE. Then, the surface of the electrode was washed with a buffer solution to remove the unreacted reagent and finish the preliminary construction. As for the original signal collection, the chip was folded as shown in Scheme 1D and filled with 50 μL of buffer solution containing luminol and H_2O_2. The potential from 0 to 0.8 V with the scanning rate of 0.1 $V \cdot s^{-1}$ and the voltage of the photomultiplier tube (PMT) at 800 V were applied to the sensing chip to achieve ECL detection. The ECL measurements were obtained and recorded as the I_0.

When the object analysis was needed, 1s0-μL sample solution was mixed with 10 μL of S2-biotin and incubated for 30 min. Subsequently, 5 units of Exo I were added into the mixture and incubated for 60 min; it was heated at 80 °C for 15 min and followed by slow cooling to room temperature. After the obtained mixture was kept at room temperature for 1 h, the analyte-triggered DNA walker was successfully prepared (Scheme 2A). Thereafter, the mixture involving the DNA walker, 10 μL of S3-DBCO, and 85 μL of 300-mM NaCl was added onto the surface of electrode and incubated for 1 h at 37 °C under slight oscillation, followed by cleaning. A prepared DNA-PtCuTNFs dispersion of 50 μL was dropped and kept reacted for 20 min. Finally, the corresponding ECL signal was measured again and denoted as *I*.

Results and discussion

Characterization of the AgMFs-PWE and PtCuTNFs

Scanning electron microscopy (SEM) was utilized to research the grown of AgMFs on the surface of bare-PWE. As shown in Fig. 1a, the bare-PWE was a rough fibrous structure with many large pores, providing a good carrier for subsequent adsorption of AgMFs. After AgMFs growing on the surface of PWE, a continuous and dense layer of microsilver was formed as shown in Fig. 1b. The high-magnification SEM image (Fig. 1C) revealed that the microsilver layer was composed of numerous floriform microparticles with rough surface, improving the conductivity and enlarging specific surface area of the paper electrode. Additionally, elemental mapping was employed to distinguish the distribution of AgMFs-PWE. As shown in the image presented in Fig. 1d, the C and O elements scattered all over the places, proving the existence of paper fibers. The Ag element signal could be found on the fibers, thus confirming the formation of AgMFs-PWE. The X-ray diffraction (XRD) patterns of the bare-PWE and AgMFs-PWE were also obtained and shown in Fig. 2a. The peaks at 2θ = 38.23, 44.46, 64.63, and 77.63 could

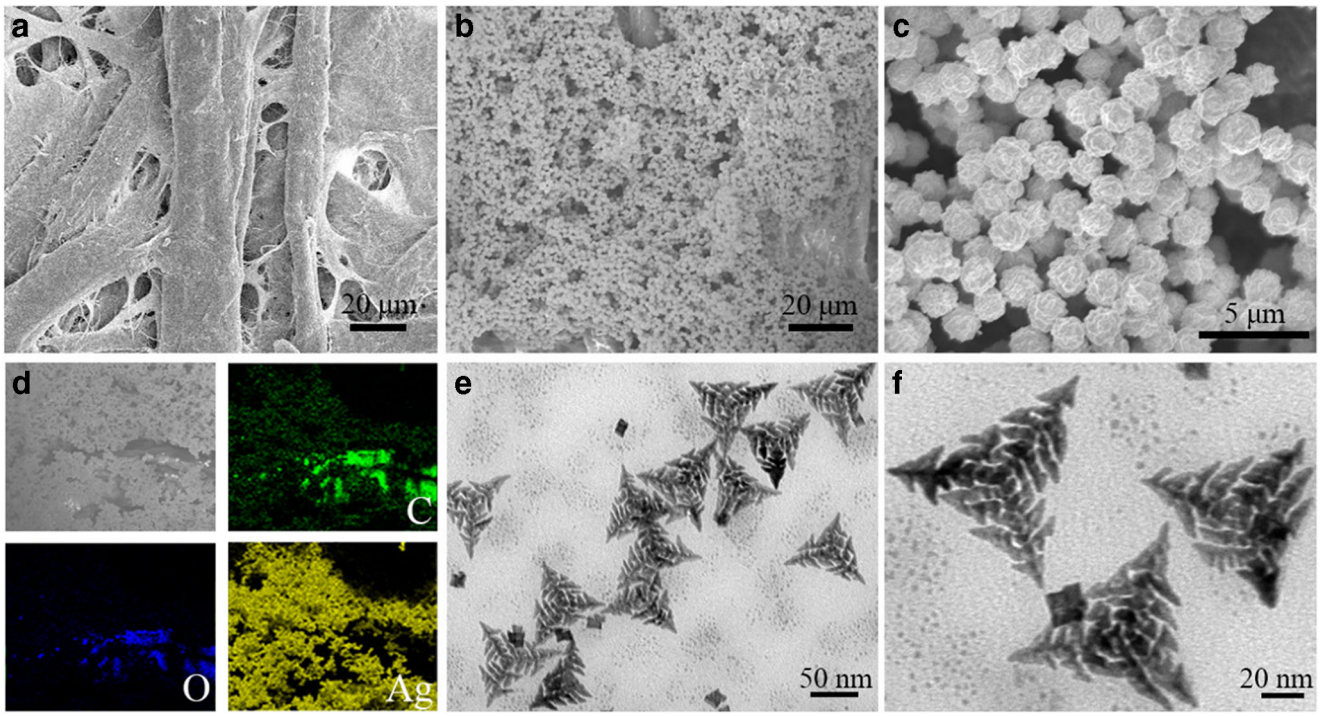

Fig. 1 (**a**) SEM image of the bare-PWE. (**b** and **c**) SEM images of AgMFs-PWE at different magnifications. (**d**) The element mapping of AgMFs-PWE. (**e** and **f**) TEM images of PtCuTNFs at different magnifications

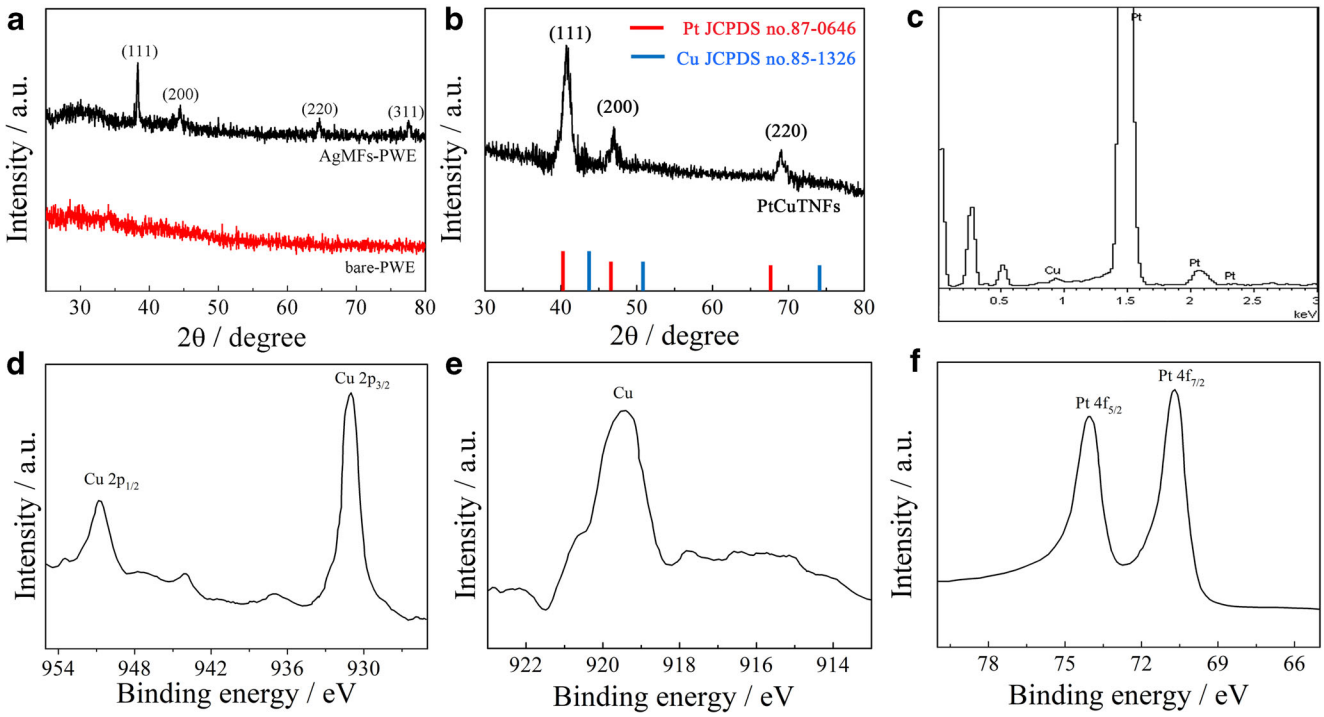

Fig. 2 The XRD of bare-PWE and AgMFs-PWE (**a**) and PtCuTNFs (**b**). The EDS of PtCuTNFs (**c**). XPS spectra of Cu 2p band (**d**), Cu LM2 band (**e**), and Pt 4f band (**f**)

be indexed to 111, 200, 220, and 311 planes, which was in good agreement with AgMFs.

Characterization of the morphology and the internal structure of nanocrystals were essential to validate the synthesis of nanoparticle. Therefore, the representative transmission electron microscopy (TEM) image of PtCuTNFs was investigated. As shown in the Fig. 1e PtCuTNFs exhibited a tripyramidal structure with irregular distribution and edge length of 110 nm. The magnified TEM image (Fig. 1f) clearly showed that these nanoparticles were an ordered hierarchical structure unit with multiple branch tips. The ordered cross-linked branched chain connecting each frame unit could effectively promote the electron transfer between the oxidation site and the reduction site in the redox reaction, so that it had good catalytic performance. Figure 2c showed the corresponding energy dispersive spectrometer (EDS) of the PtCuTNFs nanocomposite, which consisted of Pt and Cu elements, testifying the successful preparation of the material. X-ray photoelectron spectroscopy (XPS) spectra of the PtCuTNFs further verified the result (Fig. 2d–f, the detailed description was represented in the Supporting Information). Otherwise, XRD spectrum measurement was performed to characterize the structure of PtCu nanocrystals. According to Fig. 2b, PtCuTNFs were inferred as a face-centered cubic (fcc) structure on account of the diffraction peak locating between those of pure fcc Pt (JCPDS no. 87–0646) and pure fcc Cu (JCPDS no. 85–1326).

Stepwise characterization of the sensing interface

Electrochemical impedance spectroscopy (EIS) is a widespread and powerful tool for characterizing stepwise modified electrode and recording the changes of the sensing interface properties during the assembly process. Its spectra were acquired in a background solution of 5.0 mM $[Fe(CN)_6]^{3-/4-}$ solution containing 0.1 M KCl. It can be found from Fig. 3a that bare-PWE displayed a relatively minor semicircle diameter of EIS Nyquist plot (curve a), indicating a low electron-transfer resistance (R_{et}). After AgMFs growing on the PWE, a decreased diameter of the semicircle (curve b) was observed due to the excellent electrical conductivity of the AgMFs. When the strands S1 were fixed on the electrode (curve c), the R_{et} value was significantly enhanced, because the negatively charged phosphate groups on oligonucleotides increased electron transfer distance and hindered the electron transfer. Sequentially, when MCH was attached on the electrode (curve d), the R_{et} value was increased. After the movement of DNA walker on the electrode surface, DNA-PtCuTNFs with massive DNA strands was immobilized on the surface of the electrode, leading to a higher R_{et}. This phenomenon was attributed to the steric hindrance of DNA-PtCuTNFs. These changes obviously indicated the successful fabrication of paper-based ECL biosensor for detection of SA. The result was also verified by cyclic voltammetry (CV), which the peak currents and voltage displacement reflect the electron transfer of the sensing surface (Fig. 3b).

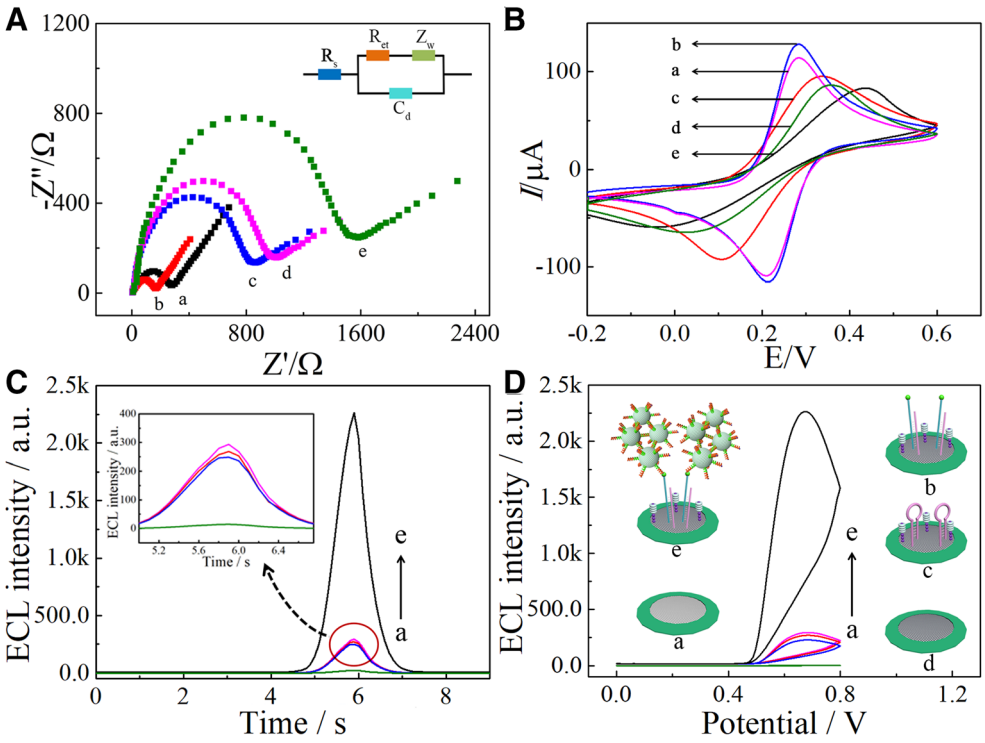

Fig. 3 EIS (**a**) and CV (**b**) of different modified electrodes in 5.0 mM $[Fe(CN)_6]^{3-/4-}$ solution containing 0.1 M KCl; the ECL responses (C and D) of (**a**) bare-PWE, (**b**) AgMFs-PWE, (**c**) S1/AgMFs-PWE, (**d**) MCH/S1/AgMFs-PWE, (**e**) DNA-PtCuTNFs/MCH/S1/AgMFs-PWE

Possible mechanism of the proposed ECL biosensor

The detailed signal amplification mechanism of the proposed ECL biosensor was shown in Scheme 2A. The ECL signal was firstly amplified by the DNA walker. Concretely, target SA was identified and assembled with sufficient S2-biotin to form the DNA walker via biotin-streptavidin interaction. In order to acquire the pure DNA walker to trigger the following assembly, Exo I was employed for the decomposition of the dissociative the S2-biotin. However, the S2 assembled on DNA walker would not be disintegrated by reason of terminal protection that small-molecule-labeled DNA was protected from decomposition by nucleases when the small-molecule moiety was bound to its protein target. With the addition of the DNA walker onto the surface of AgMFs-PWE, S1 with hairpin structure was opened and continued to hybridize with S3, releasing the S2 of DNA walker. The released S2 would participate in next cycle with adjacent S1, which realized the movement of DNA walker, leading to amplification of signal. Secondly, reticular DNA-PtCuTNFs employed as effective nano-catalyst was immobilized on the electrode via click chemistry as shown in Fig. S6, leading to the further amplification of the signal of lumino-H_2O_2 system. For comparing and demonstrating the superiority of the biosensor enhanced by the reticular nanostructure, the ECL responses of the same batch of biosensors with different signal labels were investigated in the presence of 1 nM of target. As shown in Fig. S7, the signal of the biosensor directly incubated with PtCuTNFs via the Pt-N bonding between amidogen-modified S3 and PtCuTNFs (curve b) was higher than that of unmodified biosensor (curve a). It could be explained that PtCuTNFs possessed superior catalytic property due to the synergy between alloying atoms and high refractive index facets. Its ordered crosslinking nanostructure composed of interlinked branches units not only provided abundant redox sites for promoting the transfer of electrons but enhanced the specific surface area, accelerating the decomposition of H_2O_2 to produce reactive oxygen species, which could further react with luminol to generate ECL emission. Futhermore, when the biosensor modified with the reticular DNA-PtCuTNFs, the signal obtained further amplification (curve c), indicating that the immobilized amount of PtCuTNFs was obviously improved by forming the reticular nanoarchitectures. Otherwise, for the sake of further displaying the superiority of the materials, the performance comparison with the materials previously reported was done as shown in the Table S2. The results gave a further verification on excellent performance of the reticular DNA-PtCuTNFs.

To investigate the feasibility of the signal amplification mechanism, the ECL curves of the electrode assembled step by step was explored in Fig. 3c. An extremely small signal was exhibited on the pretreated bare-PWE (curve a). With the AgMFs grown on surface of the PWE (curve d), the perk current was enhanced due to the excellent electro-catalysis of the AgMFs. When the S1 and MCH were fixed on the AgMFs-PWE (curve c), the ECL response appeared a slight decline as a result of poor electroconductibility and stereohindrance effect. After the movement of the DNA walker powered by SDR, the peak current decreased again (curve b). Subsequent assembling of DNA-PtCuTNFs caused dramatic enhancement of ECL signal, which was attributed to its superior catalytic property (curve e).

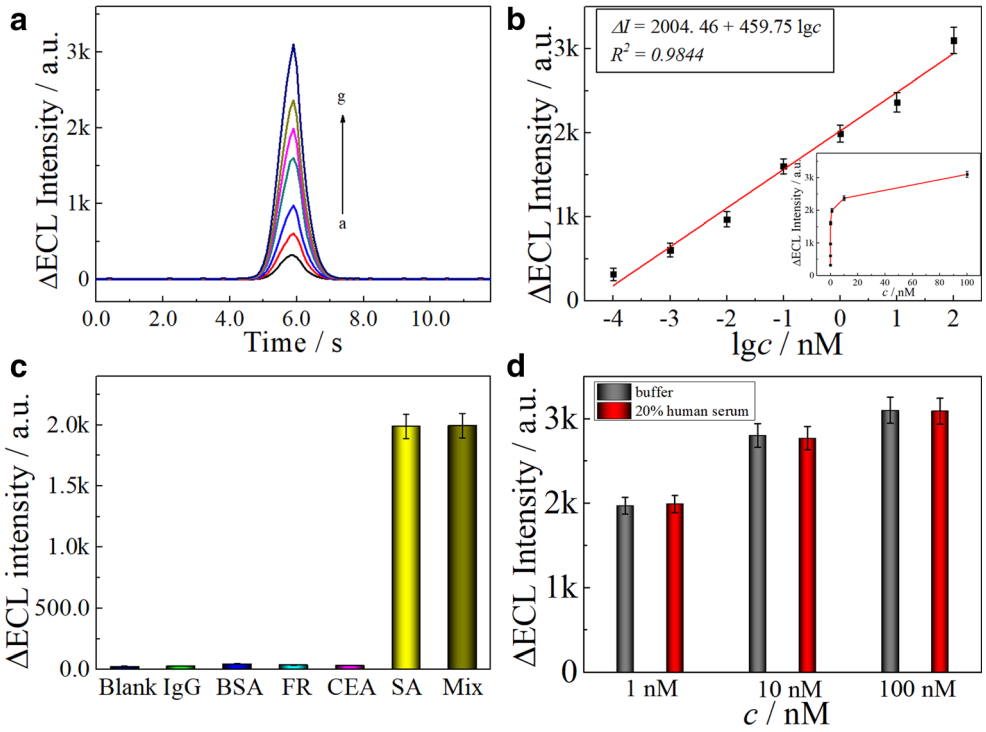

Fig. 4 (A) ECL intensity of the biosensors incubated with 0.1 pM to 0.1 μM SA (a-h): (a) 0.1 pM, (b) 1 pM, (c) 10 pM, (d) 0.1 nM, (e) 1 nM, (f) 10 nM, and (g) 100 nM. (B) Calibration plot of ECL intensity vs the logarithm of SA concentration. (C) Selectivity of the biosensor with different analytes. (D) Comparison of SA detection in buffer and 20% serum samples by the proposed paper-based biosensor

Meanwhile, the results were also verified by the ECL signal intensity-voltage curve (Fig. 3d), demonstrating the feasibility of the proposed ECL biosensor.

Analysis performance of the device

Under the optimized conditions (the detailed procedure was represented in the Supporting Information), a series of concentrations of SA were detected to research the performance of the proposed sensor. As shown in Fig. 4a and b, the ECL intensity ($\Delta I = I - I_0$) was found to be logarithmically related to the SA concentrations in the range from 0.1 pM to 0.1 μM. The regression equation was expressed as $\Delta I = 2004.46 + 459.75 \lg c$ (c is the concentration of SA) with a detection limit of 33.4 fM at 3σ as well as a good linear correlation coefficient of 0.9844. By contrast with previously reported works (Table 1), the proposed device presented a relatively a lower detection limit. However, the detection range is not very wide. And the proposed paper-based chip is disposable and cannot be reused. These limitations still need to be further explored.

Selectivity, reproducibility, and stability

In order to evaluate the selectivity of the proposed strategy, the ECL responses of the biosensor to the high concentrations (10 nM) of carcino-embryonic antigen (CEA), immunoglobulin G (IgG), bovine serum (BSA), and folate receptor (FR) were monitored under the same procedures, and the results were shown in Fig. 4c. It was found that the ECL intensity incubated with these potential interfering substances was almost the same as that of blank. Furthermore, the ECL intensity obtained from the mixture containing SA (1 nM), CEA (10 nM), IgG (10 nM), BSA (10 nM), and FR (10 nM) presented no obvious change

Table 1 Comparison of the proposed aptasensor with other reported aptasensors for SA

Analytical method	Linear range	Detection limit/nM	reference
Fluorescence	0.1–25 nM	–	[1]
Electrochemical	1.96 pg/mL–1.96 μg/mL	0.65 pg/mL	[30]
Fluorescence	2.0–100 ng/mL	1.6 ng/mL	[2]
Charge transfer resistance	0.1 pM–1 nM	10 fM	[31]
ECL	0.1 pM–0.1 μM	33.5 fM	This work

comparing with that of the 1 nM of target, indicating that the developed ECL biosensor possessed excellent selectivity.

Moreover, the reproducibility was another important criterion for the biosensor. Herein, it was tested by monitoring the ECL intensity of five different biosensors incubated with the same concentration of target. According to the result, intra-assay and inter-assay relative standard deviation of the paper-based device were less than 3.6 and 4.1%, respectively, indicating a good reproducibility of the proposed biosensor for SA assay. After the device stored at 4 °C for 3 days, no detectable loss on the ECL signal intensity was detected. And it remained 94.5% of the initial responses after 3 weeks, suggesting the attractive stability of the constructed sensors.

Detection of SA in human serum samples

To verify the practical applicability of the constructed paper-based ECL biosensor, the recovery experiment was performed by detecting SA in human serum samples according to the reported approaches [2]. The 20% serum solution was firstly obtained by diluting human serum 5 times with Tris-HCl buffer. And then it is used as a buffer solution to detect SA. The detailed detection process was the same as in the Tris-HCl buffer. As shown in Fig. 4d, the signal intensity measured in the 20% serum samples was almost the same as the pure buffer. The recovery of target was about 98.35–106.5% in serum samples, and the relative standard error was within acceptable range, which proved the developed biosensor had precision and accuracy, indicating the potential application towards SA assay in practical samples.

Conclusions

We have developed a 3D adjustable and foldable paper-based ECL biosensing platform with the function of automatic cleaning of electrode and acquisition of ECL signal by using luminol-H_2O_2 system as luminophor for ultrasensitive SA assay. AgMFs with a large specific surface area and excellent conductivity were exploited to construct the paper-based sensing platform to improve its properties. The DNA walker could continue to walk by the propelling of SDR, which could improve the selectivity and sensitivity. The multiple movements of DNA walker were propitious to the improvement of sensitivity. Reticular DNA-PtCuTNF, as a mimic peroxidase, acted as the accelerator of luminol to enhance the ECL signal. Moreover, the proposed ECL biosensor offered a new ECL route to highly selective and sensitive detection of protein, which has great significance to the development of its industrialization.

Funding This work was supported by the National Natural Science Foundation of China (21775055, 21874055, 51872121), a project of Shandong Province Higher Educational Youth Innovation Science and Technology Program (2019KJC016), the Project of "20 items of University" of Jinan (2018GXRC001), the Taishan Scholars program and the Case-by-Case Project for Top Outstanding Talents of Jinan.

Compliance with ethical standards

Conflict of interest All the authors declare no conflicts of interest with this work.

References

1. Li F, Zhang H, Lai C, Li XF, Le XC (2012) A molecular translator that acts by binding-induced DNA strand displacement for a homogeneous protein assay. Angew Chem Int Ed 51:9317–9320
2. Zhang Z, Xia X, Xiang X, Huang F, Han L (2017) Conjugated cationic polymer-assisted amplified fluorescent biosensor for protein detection via terminal protection of small molecule-linked DNA and graphene oxide. Sens Actuators B Chem 249:8–13
3. Xiang X, Shi J, Huang F, Zheng M, Deng Q, Xu J (2015) MoS_2 nanosheet-based fluorescent biosensor for protein detection via terminal protection of small-molecule-linked DNA and exonuclease IIIaided DNA recycling amplification. Biosens Bioelectron 74:227–232
4. Petrlova J, Masarik M, Potesil D, Adam V, Trnkova L, Kizek R (2007) Zeptomole detection of streptavidin using carbon paste electrode and square-wave voltammetry. Electroanal 19:1177–1182
5. Ma MN, Zhuo Y, Yuan R, Chai YQ (2015) New signal amplification strategy using semicarbazide as co-reaction accelerator for highly sensitive electrochemilumin-escent aptasensor construction. Anal Chem 87:11389–11397
6. Liu Y, Lei J, Huang Y, Ju H (2014) "Off-on" electrochemiluminescence system for sensitive detection of ATP via target-induced structure switching. Anal Chem 86:8735–8741
7. Peng H, Huang Z, Wu W, Liu M, Huang K, Yang Y, Deng H, Xia X, Chen W (2019) Versatile high-performance electrochemiluminescence ELISA platform based on a gold nanocluster probe. ACS Appl Mater Interface 11(27):24812–24819
8. Fan Z, Lin Z, Wang Z, Wang J, Xie M, Zhao J, Zhang K, Huang W (2020) Dual-wavelength electrochemiluminescence ratiometric biosensor for NF-κB p50 detection with dimethylthiodiaminoterephthalate fluorophore and self-assembled DNA tetrahedron nanostructures probe. ACS Appl Mater Interfaces 12:11409–11418
9. Ye T, Zhang Z, Yuan M, Cao H, Yin F, Wu X, Xu F (2020) An all-in-one aptasensor integrating enzyme powered three-dimensional DNA machine for antibiotic detection. J Agr Food Chem 68:2826–2831
10. Li PX, Wei M, Zhang F, Su J, Wei W, Zhang YJ, Liu SQ (2018) Novel fluorescence switch for microRNA imaging in living cells based on DNAzyme amplification strategy. ACS Appl Mater Interface 10(50):43405–43410
11. Zhao L, Sun R, He P, Zhang X (2019) Ultrasensitive detection of exosomes by target-triggered three-dimensional DNA walking machine and exonuclease III-assisted electrochemical ratiometric biosensing. Anal Chem 91:14773–14779
12. Buckland RM (1986) Strong signals from streptavidin-biotin. Nature 320:557–558
13. Zhou Y, Wang H, Zhuo Y, Chai Y, Yuan R (2017) Highly efficient electrochemiluminescent silver nanoclusters/titanium oxide nanomaterials as a signal probe for ferrocene-driven light switch bioanalysis. Anal Chem 89:3732–3738
14. Song Y, Zhang W, He S, Shang L, Ma R, Jia L, Wang H (2019) Perylene diimide and luminol as potential-resolved

electrochemiluminescence nanoprobes for dual targets immunoassay at low potential. ACS Appl Mater Interfaces 11:33676–33683
15. Tu T, Lei Y, Chai Y, Zhuo Y, Yuan R (2020) Organic dots embedded in mesostructured silica xerogel as high-performance ECL emitters: preparation and application for microRNA-126 detection. ACS Appl Mater Interfaces 12(3):3945–3952
16. Zhang H, Wang Z, Wang F, Zhang Y, Wang H, Liu Y (2020) In situ formation of gold nanoparticles decorated Ti_3C_2 MXenes nanoprobe for highly sensitive electrogenerated chemiluminescence detection of exosomes and their surface proteins. Anal Chem 92:5546–5553
17. Zheng Y, Yuan Y, Chai Y, Yuan R (2016) L-cysteine induced manganese porphyrin electrocatalytic amplification with 3D DNA-au@Pt nanoparticles as nanocarriers for sensitive electrochemical aptasensor. Biosens Bioelectron 79:86–91
18. Wang X, Luo M, Huang H, Chi M, Howe J, Xie Z, Xia Y (2016) Facile synthesis of Pt-Pd alloy nanocages and Pt nanorings by templating with Pd nanoplates. ChemNanoMat 2:1086–1091
19. Shao Q, Wang P, Zhu T, Huang X (2019) Low dimensional platinum-based bimetallic nanostructures for advanced catalysis. Accounts Chem Res 52:3384–3396
20. Yang H, Zhang Y, Li L, Zhang L, Lan F, Yu J (2017) Sudoku-like lab-on-paper cyto-device with dual enhancement of electrochemiluminescence intermediates strategy. Anal Chem 89: 7511–7519
21. Liu P, Li B, Fu L, Huang Y, Man M, Qi J, Sun X, Kang Q, Shen D, Chen L (2020) Hybrid three dimensionally printed paper-based microfluidic platform for investigating a cell's apoptosis and intracellular cross-talk. ACS Sensors 5:464–473
22. Zeng F, Duan W, Zhu B, Mu T, Zhu L, Guo J, Ma X (2019) Paper-based versatile surface-enhanced raman spectroscopy chip with smartphone-based raman analyzer for point-of-care application. Anal Chem 91:1064–1070
23. Martinez AW, Phillips ST, Butte MJ, Whitesides GM (2007) Patterned paper as a platform for inexpensive, low-volume, portable bioassays. Angew Chem Int Ed 46:1318–1320
24. Li L, Zheng X, Huang Y, Zhang L, Cui K, Zhang Y, Yu J (2018) Addressable TiO_2 nanotubes functionalized paper-based cyto-sensor with photocontrollable switch for highly-efficient evaluating surface protein expressions of cancer cells. Anal Chem 90:13882–13890
25. Cate DM, Adkins JA, Mettakoonpitak J, Henry CS (2015) Recent developments in paper-based microfluidic devices. Anal Chem 87: 19–41
26. Chang YH, Liu C, Rouvimov S, Luo T, Feng SP (2017) Electrochemical synthesis to convert a Ag film into Ag nanoflowers with high electrocatalytic activity. Chem Commun 53:6752–6755
27. Li L, Zhang Y, Zhang L, Ge S, Liu H, Ren N, Yan M, Yu J (2016) Paper-based device for colorimetric and photoelectrochemical quantification of the flux of H_2O_2 releasing from MCF-7 cancer cells. Anal Chem 88:5369–5377
28. Yang X, Sun X, Lv Z, Guo W, Du Y, Wang E (2010) Ultrasensitive nucleic acid detection using confocal laser scanning microscope with high crystalline silver dendrites. Chem Commun 46:8818–8820
29. Chen S, Su H, Wang Y, Wu W, Zeng J (2015) Size-controlled synthesis of platinum-copper hierarchical trigonal bipyramid nanoframes. Angew Chem Int Ed 54:108–113
30. Wei YP, Liu XP, Mao CJ, Niu HL, Song JM, Jin BK (2018) Highly sensitive electrochemical biosensor for streptavidin detection based on CdSe quantum dots. Biosens Bioelectron 103:99–103
31. Divya KP, Dharuman V (2017) Supported binary liposome vesicle-gold nanoparticle for enhanced label free DNA and protein sensing. Biosens Bioelectron 95:168–173